In Situ Conjugated Polyelectrolyte Formation

Mark Elbing,[†] Andres Garcia,[†] Slawomir Urban,[‡] Thuc-Quyen Nguyen,*[,†] and Guillermo C. Bazan*[,†]

Departments of Chemistry & Biochemistry and Materials, Center for Polymers and Organic Solids, University of California, Santa Barbara, California 93106-5090, and Organisch-Chemisches Institut, Westfälische Wilhelms-Universität Münster, Corrensstrasse 40, 48149 Münster, Germany

Received September 20, 2008; Revised Manuscript Received October 24, 2008

ABSTRACT: The synthesis and characterization of a conjugated polymer with a thienothiophene-bithiophene-backbone and its corresponding polyelectrolyte structure is described. The conjugated polyelectrolyte is obtained by common nucleophilic substitution in solution, as well as by exposure of films of the neutral precursor to trimethylamine gas. X-ray photoelectron spectroscopy (XPS) analysis is used to determine the extent of conversion, at least within the top 10 nm of the film. Attempts to determine hole mobilities by using steady-state current−voltage (I−V) measurements using hole-only diodes containing the conjugated polyelectrolyte films give rise to light-emitting electrochemical behavior, indicating ion motion and/or redistribution within the films. The use of a pulsed I−V method operating at frequencies higher than the ion response times allows measurements of hole mobilities and suppresses ion motion. The reported mobilities are about 3 orders of magnitude higher than those reported for other thiophene-based polyelectrolytes. Overall, these results provide a new method for incorporating conjugated polyelectrolytes into device structures under circumstances where the material is not sufficiently soluble for deposition with standard techniques such as spin-coating.

Introduction

Conjugated polyelectrolytes (CPEs) are an emerging class of organic semiconducting materials that are characterized by a π-conjugated backbone bearing pendant anionic or cationic charged groups.[1,2] These materials combine the optical and electronic qualities of conjugated polymers with the fact that the properties of polyelectrolytes can be modified by electrostatic interactions.[1,3] Charged groups render CPEs soluble in polar solvents. Water soluble systems have been exploited successfully in the development of biosensors that rely on the light-harvesting properties and facile energy transfer among electronically delocalized components.[4−8] CPEs have also recently attracted much attention as charge injection/transport layers in organic optoelectronic devices.[9−14] One significant practical aspect is that they can be used to fabricate multilayer devices by spin coating techniques.[13] Furthermore, the charges, dipoles and counterions offer the opportunity to reduce electron injection barriers from high work-function metals such as aluminum and gold. The exact mechanism of this process, however, remains under debate.[14−16] CPEs also function as single component active layers in light-emitting electrochemical cells (LECs).[17,18]

The majority of CPEs thus far used in optoelectronic devices derive from structures originally used and designed for biosensor work. There is therefore the need to examine backbone structures that incorporate molecular designs appropriate for improving electronic function, for instance, charge carrier transport. Also relevant is that information about charge carrier mobilities in CPEs is scarce at present.[19,20] Inspiration from work done with neutral conjugated polymers is a natural guiding principle to design such new CPE materials. As a motivating example, we highlight the work by McCulloch and co-workers, who described the synthesis and characterization of poly(2,5-bis(3-alkylthiophene-2-yl)thieno[3,2-*b*]thiophene) derivatives, i.e. **PBT**, which can achieve charge carrier field effect mobilities of up to 0.2−0.6 $cm^2/(V\ s)$ when incorporated into thin film transistor devices.[21] These high mobilities were achieved by processing the polymer in the mesophase to obtain a highly organized morphology.

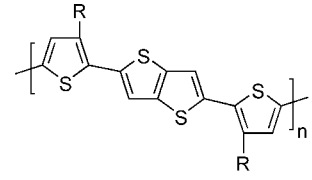

R = $C_{10}H_{21}$, $C_{12}H_{25}$, $C_{14}H_{29}$

PBT

On the basis of the considerations above, we report herein the synthesis of the cationic poly[2,5-bis(3-(10-(*N*,*N*,*N*,-trimethylammonium)-decyl)thiophen-2-yl)thieno[3,2-*b*]thiophene) dibromide] derivative, **PBT-NMe$_3$**. We recognize that the ionic counterpart **PBT-NMe$_3$** will likely lead to different thermal properties and different microstructures. We also report on the hole mobilities in **PBT-NMe$_3$** measured by using standard diode devices and a pulsed bias technique.[20] An interesting aspect of the work is that the solubility of **PBT-NMe$_3$** makes the quaternization reaction difficult in solution and does not allow for sufficiently concentrated solutions suitable for spin casting films. A new method for CPE formation was therefore developed where films of a suitable precursor are converted to **PBT-NMe$_3$** via an in situ quaternization reaction. This approach constitutes a new strategy for incorporating CPEs into optoelectronic devices.

Results and Discussion

1. Monomer and Polymer Synthesis. The synthetic pathway to the neutral precursor polymer **PBT-Br** and polyelectrolyte **PBT-NMe$_3$** is summarized in Scheme 1. The polymerization step uses a palladium-catalyzed Stille copolymerization between the alkyl-substituted 2,2′-bithiophene **1** and the thieno[3,2-*b*]thiophene unit **2**. Regioregularity in the backbone structure is achieved by the symmetry of the building blocks.[21,22] The

* Corresponding authors. Fax: 1-805-893-5270, E-mail: (T.-Q.N.) quyen@chem.ucsb.edu; (G.C.B.) bazan@chem.ucsb.edu.

[†] Departments of Chemistry & Biochemistry and Materials, Center for Polymers and Organic Solids, University of California, Santa Barbara.

[‡] Organisch-Chemisches Institut, Westfälische Wilhelms-Universität Münster.

10.1021/ma802139j CCC: $40.75
Published on Web 11/11/2008

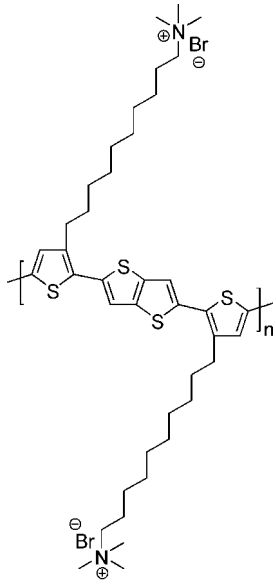

PBT-NMe$_3$

long alkyl-chains in **1** were introduced with the expectation of improving solubility. The terminal bromo-substituents on the alkyl chains allow the formation of the target polyelectrolyte **PBT-NMe$_3$** by nucleophilic displacement with a nitrogen base such as trimethylamine.[1,9,23] Alkyl-bromides are, however, not compatible with the reaction conditions for the build-up of the bithiophene unit.[24−26] Ether protecting groups, which can be converted easily to terminal bromo-groups, were thus employed.[27−29]

The synthesis of **1** begins with the preparation of (*p*-methoxyphenoxy)decyl bromide (**5**) from 1,10-dibromodecane (**3**) and 4-methoxyphenol (**4**), using a modified protocol by Ziegler et al.[27,30] Distillation and subsequent purification by chromatography gave **5** as a white solid in 59% yield. Nickel-catalyzed Kumada coupling between the Grignard reagent derived from **5** and commercially available 3-bromothiophene (**6**) gave thiophene **7** in 76% yield.[27,29] Thiophene **7** was then selectively brominated in the 2-position using *N*-bromosuccinimide (NBS). The use of THF instead of DMF, as reported in the literature,[31,32] gave better yields and provided for easier purification. The reaction mixture was slowly warmed over 67 h from 0 °C to room temperature affording **8** in 95% yield, which was used without further purification. The bithiophene core was assembled using a recently published C−H homocoupling procedure by Takahashi et al.[25,26] Thus, **8** was reacted with $PdCl_2(PhCN)_2$ (3 mol %), together with an excess of $AgNO_3$ and KF in dry DMSO at 60 °C for 21 h to give the 5,5′-homocoupled product of **8**. Purification of the crude product by chromatography afforded **9** as white solid in 77% yield. In the last step, both ether-groups of **9** were cleaved using BBr_3 in dry CH_2Cl_2 under reflux.[28] After chromatography the desired bithiophene monomer **1** was obtained as a white solid in 66% yield. The known thieno[3,2-*b*]thiophene building block **2** was synthesized starting from thieno[3,2-*b*]thiophene **10** using modified literature procedures.[33] Bromination in the 2- and 5-positions with NBS in THF at 0 °C for 21 h afforded **11** as white solid in a yield of 95% without further purification.[34] Stannylation was accomplished by bromine−lithium exchange on **11** followed by quenching with trimethyltin chloride to give **2** as white solid in a yield of 47% after purification.[35]

In analogy to the procedure reported for the synthesis of **PBT**,[21] the polymerization using **1** and **2** was done using microwave radiation.[36,37] A stepwise heating protocol (2 min at 140 °C, 2 min at 160 °C, and 25 min at 180 °C) was used with tris(dibenzylideneacetone)dipalladium and tri(*o*-tolyl)phosphine in dry chlorobenzene. The target polymer **PBT-Br** was obtained as a dark-red solid in 88% yield after precipitation into methanol, Soxhlet extraction and a second precipitation into methanol.

Nucleophilic substitution with trimethylamine to form the corresponding polyelectrolyte **PBT-NMe$_3$** proved to be difficult because of the poor solubility of the target material. Highest conversion was achieved via a three step process. First, **PBT-Br** was dissolved in THF and trimethylamine was added at −78 °C. After warming to room temperature over 16 h, the solvent was removed by distillation and a 1/1 solvent mixture of THF/ethanol was added. Trimethylamine was again added at −78 °C and the mixture was allowed to warm to room temperature overnight. In the last step pure ethanol was used as solvent. The crude product was precipitated into diethyl ether, providing **PBT-NMe$_3$** as dark-red solid.[38]

The limited solubility of **PBT-Br** and **PBT-NMe$_3$** only allowed recording ^{1}H NMR spectra. 1,2-Dichlorobenzene was found to be the best solvent for **PBT-Br** (solubility of ∼0.3 mg/mL at room temperature). In contrast, for the polyelectrolyte **PBT-NMe$_3$** DMSO is the best solvent (solubility of ∼1.8 mg/mL at room temperature), while it is completely insoluble in 1,2-dichlorobenzene. X-ray photoelectron spectroscopy (XPS) analysis of a powder sample of **PBT-NMe$_3$** gave a yield of quaternization of ∼ 80%. This yield is further confirmed by the nitrogen content found by elemental analysis of **PBT-NMe$_3$**. Quaternization yields by ^{1}H NMR spectroscopy are not accurate because of the breadth of the peaks in d_6-DMSO. Gel permeation chromatography (GPC) analysis of **PBT-Br** against polystyrene standards in THF provided $M_w \approx 13000$ and PDI = 1.8. However, it was not possible to apply GPC analysis to **PBT-NMe$_3$** possibly because of its low solubility in any solvent and adsorption to the GPC support. In the absence of these data, it is reasonable to assume comparable molecular weights for **PBT-Br** and **PBT-NMe$_3$**.

2. Thermal Properties of PBT-Br and PBT-NMe$_3$. The thermal properties of **PBT-Br** and **PBT-NMe$_3$** were examined by thermal gravimetric analysis (TGA) and differential scanning calorimetry (DSC). DSC studies were of interest, since the related neutral **PBT** counterparts show liquid-crystalline phases that are important for processing the films and achieving large charge carrier mobilities.[21,39−41] For example, in the case of the **PBT** derivative with C_{10}-alkyl chains, one observes thermal transitions at approximately 170 °C upon heating and 140 °C upon cooling. The enthalpy of 13 J g^{-1} of the cooling transition indicates the presence of a liquid-crystalline mesophase.[21]

For **PBT-Br**, the decomposition onset was found at ∼250 °C and only 5% weight loss was observed by ∼340 °C by TGA, thus demonstrating good thermal stability. The onset decomposition temperature was used as the upper limit for the DSC studies (Figure 1A), which showed a broad transition with a maximum at 179 °C in the heating cycle and 140 °C in the cooling cycle. The enthalpy upon cooling was determined to be ∼1 J g^{-1}. The smaller transition enthalpy of **PBT-Br** relative to **PBT** (13 J g^{-1}) suggests different mesophases.

In the case of **PBT-NMe$_3$**, the TGA shows an initial weight loss of about 2% up to 100 °C indicating the removal of water. This amount roughly corresponds to one molecule of water per repeat unit. After the initial loss of water the onset of decomposition was found at ∼220 °C and 5% weight loss was observed at ∼250 °C by TGA, thereby demonstrating good thermal stability. In the first heating cycle of the DSC the evaporation of water becomes evident (Figure 1B).[38] Subsequent heating and cooling cycles within 50 to 220 °C do not show any transitions. Presumably, **PBT-NMe$_3$** does not show any liquid-crystalline transitions, since the forces between chains

Scheme 1. Synthetic route to monomers 1 and 2 and the neutral polymer PBT-Br together with the corresponding polyelectrolyte PBT-NMe$_3$[a]

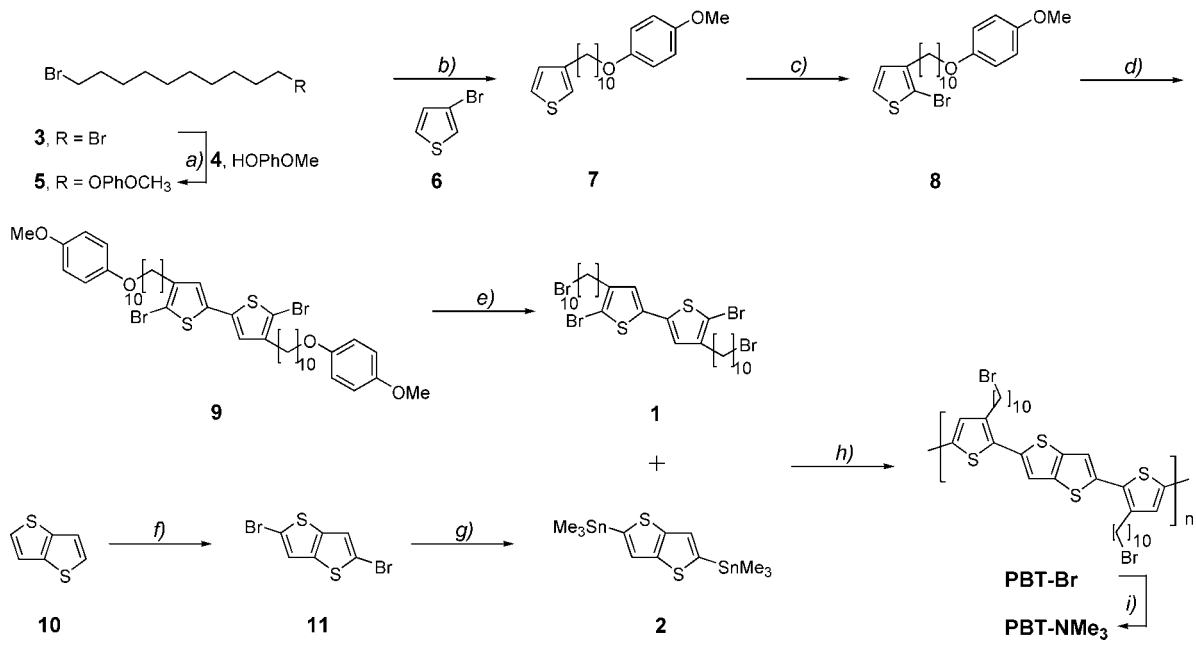

[a] Key: (a) KOH/MeOH, MeOH/CH_3COCH_3, reflux (RF), 30 h, 59%; (b) (1) Mg, Et_2O, 3 h; (2) [Ni(dppp)Cl_2], Et_2O, RF, 19 h, 76%; (c) NBS, THF, 0 °C to room temperature (RT), 67 h, 95%; (d) $PdCl_2(PhCN)_2$, KF, $AgNO_3$, DMSO, 60 °C, 21 h, 77%; (e) BBr_3, CH_2Cl_2, RF, 2 h 15 min, 66%; f) NBS, THF, 0 °C to RT, 21 h, 95%; (g) (1) *n*-BuLi, Et_2O, 0 °C, 20 min; (2) Me_3SnCl, Et_2O, 0°C, 2 h, 47%; (h) [$Pd_2(dba)_3$], P(*o*-tolyl)$_3$, ClC_6H_5, μW (2 min 140°C, 2 min 160°C, 25 min 180°C), 88%; (i) (1) NMe_3, THF, −78°C to RT, 16 h; (2) NMe_3, THF/EtOH, −78°C to RT, 16 h; (3) NMe_3, EtOH, −78 °C to RT, 16 h, 83%.

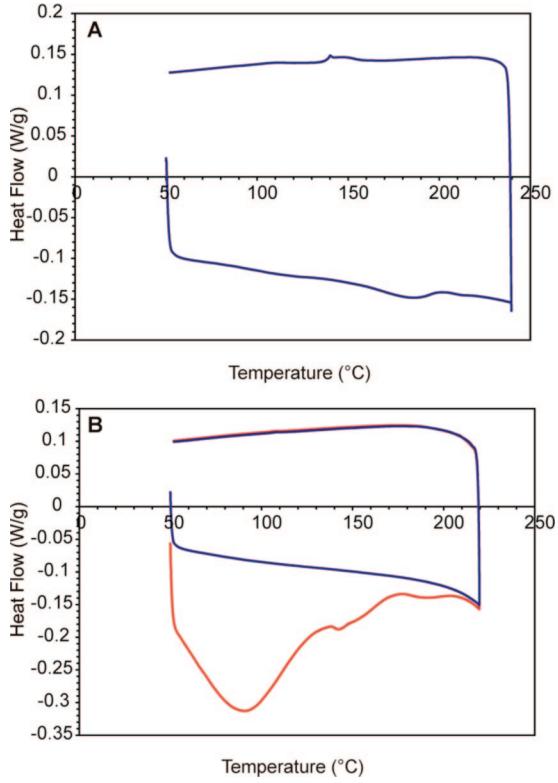

Figure 1. DSC curves of (A) **PBT-Br** during the third heating/cooling cycle; and (B) **PBT-NMe$_3$** during the first (red) and the second (blue) heating/cooling cycle. Scan rate: 5 °C/min.

are modified considerably by the presence of the ionic groups, as compared to the neutral counterparts **PBT** or **PBT-Br**.

3. In Situ Polyelectrolyte Formation. Good quality thin films that are homogeneous and pinhole free are required for the examination of charge transport under conditions relevant to device fabrication. Unfortunately, **PBT-NMe$_3$** is soluble to concentration ranges useful for spin-casting (>0.5% w/v) only in DMSO, which in our experience does not yield good quality films. It is useful to point out here that the number of charges/formula weight of the repeat unit is much smaller than in previously used CPEs. The charge density along the backbone appears to be insufficient to prevent aggregation due to the propensity of chains to come together in polar solvents.[42] Similarly, the ionic component prevents good solubility in nonpolar media. These are the same factors that prevent complete quaternization by solution methods.

Presented by the limitations discussed above, we decided to study direct polyelectrolyte formation in **PBT-Br** films by exposure to NMe_3 gas. Both poly(3,4-ethylenedioxythiophene) poly(styrenesulfonate) (PEDOT:PSS) treated ITO and quartz slides were used as substrates in view of subsequent examinations of electronic and optical properties. Films of the neutral precursor were spin-coated at 80 °C from 2% (w/v) 1,2-dichlorobenzene solutions at 800 rpm, yielding approximately 80 nm thick films. One set of precursor films was thermally annealed at 190 °C for 20 min followed by cooling at 3 °C/min, to probe whether thermal history and concomitant changes in morphology would influence quaternization efficiencies. These heated films will be subsequently referred to as "annealed". Quaternization was accomplished by exposure to ~1 atm NMe_3 at room temperature for either 2 or 20 h.

Figure 2 shows a summary of high-resolution XPS scans as a function of film history. Peaks due to Br 3d at binding energies between 70 to 72 eV are observed for **PBT-Br** films that were not treated with NMe_3, whether the films were thermally annealed or not. This binding energy corresponds to a bromide-substituent on an alkyl-chain.[43] After two hours of exposure to NMe_3 a new additional peak at binding energies between 66 to 69 eV begins to emerge. This peak can be attributed to a bromide anion with tetraalkylammonium counterions.[43] The S

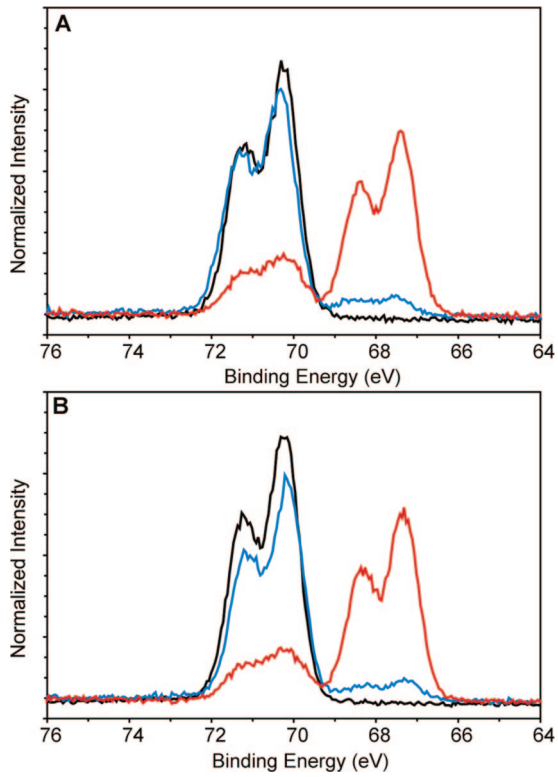

Figure 2. XPS of (A) nonannealed films of the neutral precursor (**PBT-Br**) (black), after exposure to NMe_3 for 2 h (blue) and after exposure to NMe_3-gas for 20 h (red) and (B) annealed films of the neutral precursor (**PBT-Br**) (black), after exposure to NMe_3 for 2 h (blue) and after exposure to NMe_3 for 20 h (red).

2s signals were used for normalization of the intensity signals, since no change in composition of sulfur occurs in the polymer upon reaction with trimethylamine. The relative conversion to the CPE was determined by integration of the areas of the two lower and higher binding energy Br 3d signals. For films without heat treatment a percentage of ~6% (Figure 2A) bromide content and for annealed films a percentage of ~7% (Figure 2B) after 2 h of exposure has been calculated. The yield of conversion to the tetraalkylammonium bromide ($RNMe_3^+Br^-$) increases considerably after 20 h of NMe_3 treatment, to ~75% and ~77% for nonannealed and annealed films, respectively. Thus, the XPS results indicate that the in situ polyelectrolyte formation takes place by exposure to NMe_3. The bromide content increases considerably with longer exposure time. It should also be noted that XPS is a surface-sensitive technique that only probes the first ~10 nm of the film.[44] Characterization of the total conversion in the polymer film, and whether there is a concentration gradient across the layer cannot be obtained from this information.

4. Film Morphology. The influence of annealing on the microstructure[39,40] and the electronic properties of **PBT**[21] prompted us to examine whether similar effects could be observed in **PBT-Br** and **PBT-NMe$_3$**. Images obtained by atomic force microscopy (AFM) of **PBT-Br** films with different thermal histories are shown in Figure 3A. In addition, AFM images obtained after exposure to NMe_3 for 20 h for both types of films are presented in Figure 3B. The surface roughness of as-spun and annealed **PBT-Br** films are ~2 nm and ~1 nm, respectively. Lamella-like structures are present in the annealed films, as commonly observed for polythiophene-based films.[45,46] These nanocrystalline lamella are usually the result of $\pi-\pi$ interactions between conjugated backbones in adjacent chains.[45−47] For nonannealed and annealed films the roughness was similar before and after exposure to NMe_3. Figure 3B also reveals that upon in situ **PBT-NMe$_3$** formation the lamella-like morphology of annealed films is changed to a certain extent. This structural feature is still visible after quaternization, but the lamella appear to be broken down into smaller segments. The quaternization reaction in exposed films occurs at the terminal position of the alkyl chains, which may lead to a different spatial arrangement of the alkyl-chains due to the presence of charged groups. From Figure 3, we surmise that such chemical modifications, at least in the case of **PBT-NMe$_3$**, alter the precise microcrystalline order, but general surface features are broadly maintained.

5. Optical Properties. UV−vis absorption spectroscopy allows obtaining information on the electronic structure, in particular the frontier orbitals ($\pi-\pi^*$ transitions), of conjugated polymers and to give qualitative estimates of effective conjugation lengths.[48] Figure 4A shows the UV−vis absorption spectra of **PBT-Br** and **PBT-NMe$_3$** in 1,2-dichlorobenzene and DMSO, respectively. The solution spectra of both compounds display essentially the same absorption maxima (λ_{max}): for **PBT-Br** λ_{max} = 476 nm and for **PBT-NMe$_3$** λ_{max} = 477 nm.

Figure 4B shows the UV−vis spectra of **PBT-Br** films on quartz slides, together with the corresponding spectra for in situ formed **PBT-NMe$_3$** films. All the λ_{max} values in Figure 4B are red-shifted compared to the solution measurements, as is often observed for conjugated polymer films.[49−51] For nonannealed **PBT-Br** films λ_{max} = 542 nm. Thermal treatment provides for a slight shift of λ_{max} to 546 nm and results in a broader absorption band. The red-shift together with the presence of a broader band suggests a longer conjugation length for the annealed films compared to as-spun films. Previous work shows that λ_{max} = 547 nm for **PBT**, indicating that there are no large differences in the optical properties of **PBT** and **PBT-Br**. Figure 4B also shows that the λ_{max} values of **PBT-NMe$_3$** films depend on the thermal history. After 20 h of NMe_3 exposure, nonannealed films show λ_{max} = 532 nm, while annealed films show λ_{max} = 522 nm. Thus, in situ formation retains the thermal history of the samples. Besides, the UV−vis spectra suggest that the microstructure in exposed films differs to a certain extent from the structure of the neutral, unexposed films possibly due to a change of conjugation length.[39,50]

The PL spectra of **PBT-Br** and **PBT-NMe$_3$** in solution are shown in Figure 4C. Upon excitation at its absorption maximum **PBT-Br** in 1,2-dichlorobenzene exhibits an emission maximum (λ_{em}) at 579 nm. The PL spectrum of **PBT-NMe$_3$** in DMSO solution shows essentially the same emission spectrum. The PL quantum yield (Φ_{PL}) was determined against rhodamine as the standard. **PBT-Br** has a Φ_{PL} of 32% in 1,2-dichlorobenzene, while **PBT-NMe$_3$** has a slightly lower Φ_{PL} of 28% in DMSO. For oligo- and polythiophenes PL quantum yields in solution usually range from 10% to 40%.[52,53] Therefore, **PBT-Br** and **PBT-NMe$_3$** show quantum yields as commonly reported for related polymeric and oligomeric structures.

Figure 4D shows the PL spectra from thin films. Compared to the solution measurements, the PL maxima are shifted to longer wavelengths. Nonannealed **PBT-Br** films exhibit an emission maximum at 679 nm, with a shoulder at 641 nm. A similar spectrum was found for annealed films (λ_{em} = 680 nm with a shoulder at 644 nm). After 20 h of exposure, λ_{em} = 677 nm together with a second maximum at to λ_{em} = 633 nm for nonannealed films. In contrast, exposure of annealed films gives a blue-shift to λ = 619 nm, that is, a hypsochromic shift of 25 nm is observed. A shoulder reminiscent of the second maximum seen in the neutral precursor is found at λ = 670 nm. These data further confirm that in situ formation retains the thermal history of the sample, but also leads to alteration in the microstructure of exposed compared to neutral, unexposed films as already seen in the AFM and UV−vis investigations.

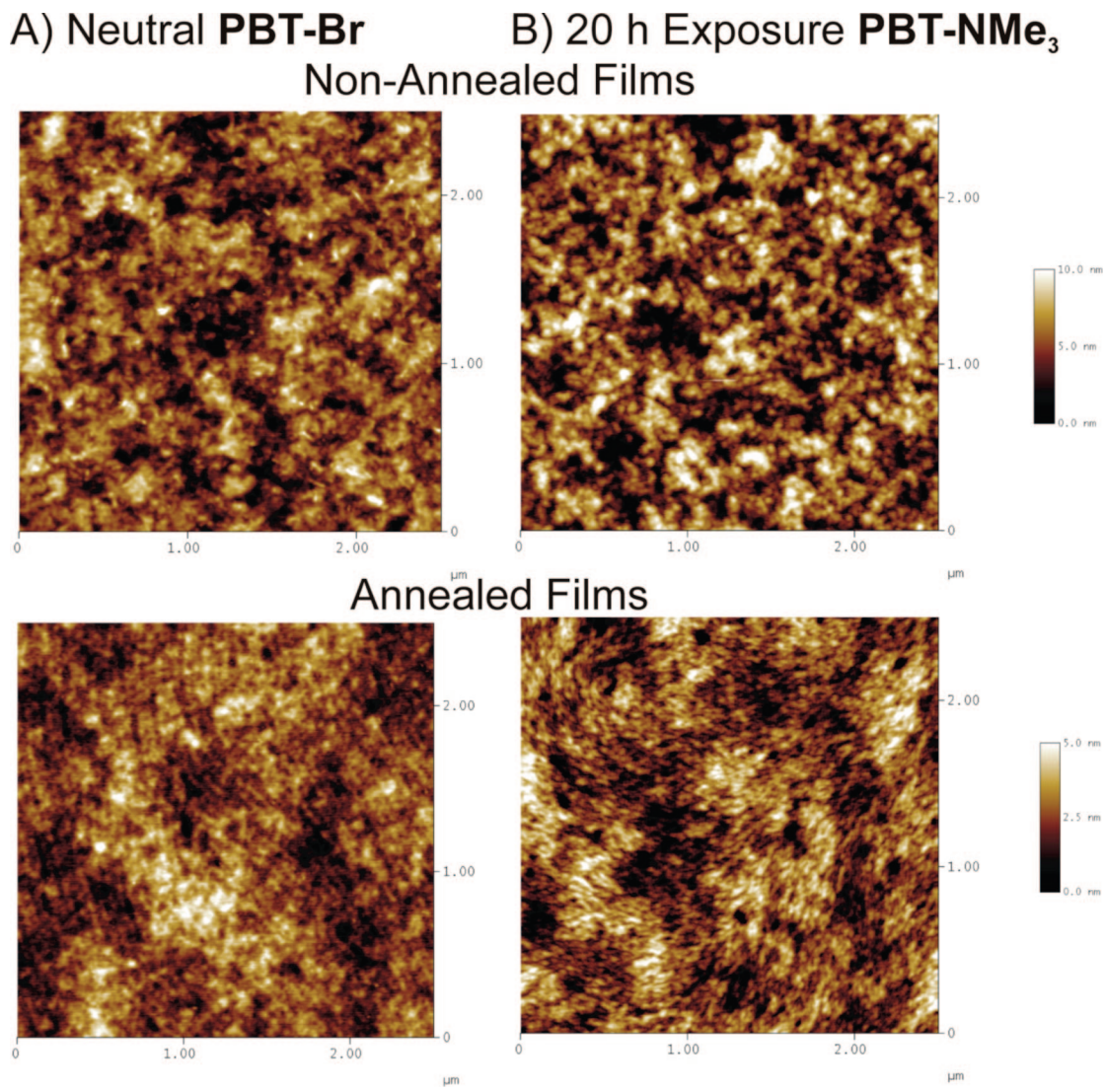

Figure 3. AFM images of nonannealed and annealed films of **PBT-Br** (A) before exposure; (B) after 20 h of exposure to NMe_3.

6. Charge Transport Properties. Hole-only diodes were fabricated by spin coating 40 nm of PEDOT:PSS on ITO substrates followed by 80 nm of **PBT-Br** with or without heat treatment and trimethylamine exposure similar to films used for spectroscopic measurements. Finally, 100 nm of gold thermally evaporated at pressures of 10^{-7} torr using a shadow mask. The energy difference between the work-functions of the two electrodes (ITO, ~5.2 eV,[54] and gold, ~5.1 eV)[55] and the **PBT-Br** LUMO[56] is anticipated to yield, in the absence of interfacial effects, barriers to electron injection of approximately $\sim 2 \pm 0.5$ eV. Therefore, devices with neutral **PBT-Br** are hole-only diodes and hole mobilities can be calculated using the space-charge limited current (SCLC).[57]

The current density (J) versus bias plots of hole-only diodes containing nonannealed (black) and annealed (red) **PBT-Br** films are shown in Figure 5. The hole mobility (μ) of nonannealed devices was estimated to be 2.9×10^{-5} cm^2/(V s). For annealed films $\mu = 8.7 \times 10^{-5}$ cm^2/(V s), an increase of approximately a factor of 3 was observed. McCulloch and co-workers reported a large increase in hole mobility for **PBT** upon annealing over the liquid-crystalline temperature.[21] However, these measurements were done within a thin-film transistor geometry, where transport parallel to the substrate is probed. In contrast, in the diode structure used here charge carrier mobilities perpendicular to the substrate are measured. Overall, the formation of ordered regions shown in Figure 3 did not significantly improve hole mobilities in ~120 nm-thick diodes. The measured hole mobilities of **PBT-Br** are comparable to those reported for hole-only diodes containing poly(3-hexylthiophene), a commonly used high mobility conjugated polymer.[54]

The effect of in situ transformation to **PBT-NMe$_3$** on device performance was of particular interest to evaluate the potential of these materials to function as electron transport/electron injection layers. Gold electrodes were deposited subsequent to 20 h of NMe_3 exposure. The measurements, summarized in Figure 6, show that when a bias was applied under conventional conditions, i.e., a steady increase of the voltage, hysteresis of J and the emission of light are observed. As shown in Figure 6B, both devices with nonannealed or annealed films basically show the same turn-on voltage of ~3 V (luminance >0.1 Cd/m^2). Importantly, light emission can only occur when both holes and electrons are injected into the organic layer. Therefore, the device with **PBT-NMe$_3$** shows characteristics of a light emitting electrochemical cell (LEC),[18,58] in which ions are available to migrate and thereby screen the electric field. LEC behavior was not detected in unexposed devices. This observation indicates the presence of mobile ions in the device, which is most likely due to the charge compensating bromide counterions.

While the above results show the potential for in situ formation of conjugated polyelectrolytes to change the charge injection characteristics at metal/organic interfaces, the ease of electron injection prevented accurate evaluation of hole mobili-

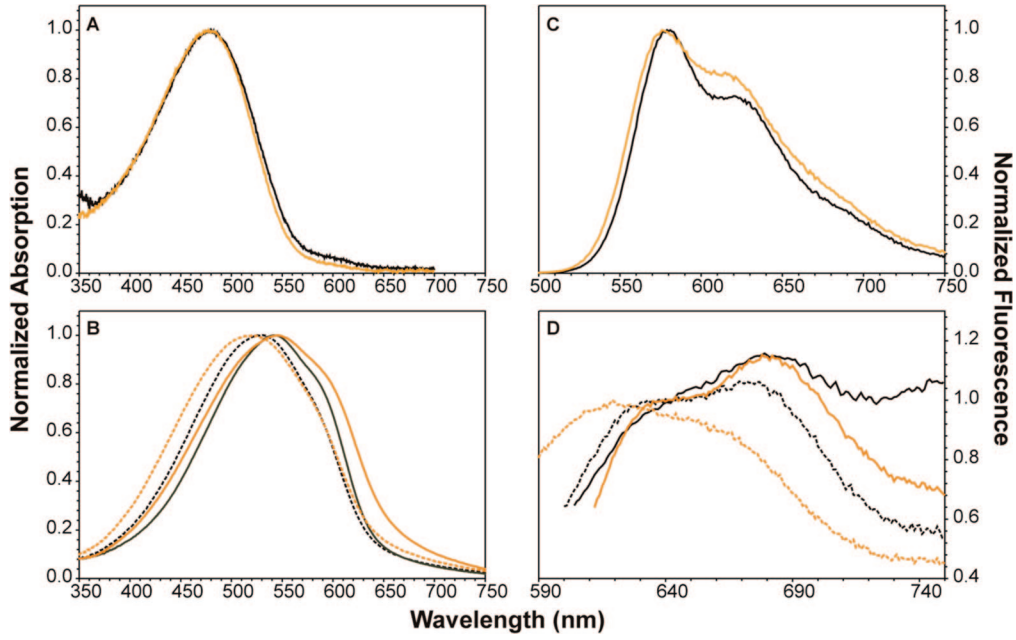

Figure 4. (A) UV−vis absorption spectra of **PBT-Br** (black) and **PBT-NMe$_3$** (orange). For **PBT-Br** $\sim 10^{-5}$ M solutions in 1,2-dichlorobenzene, for **PBT-NMe$_3$** $\sim 10^{-5}$ M solutions in DMSO were used. (B) UV−vis absorption spectra of nonannealed films of **PBT-Br** (black), **PBT-Br** after 20 h (dashed black) of exposure to trimethylamine gas, and the corresponding spectra of annealed films of **PBT-Br** (orange), **PBT-Br** after 20 h (dashed orange). (C) PL spectra of **PBT-Br** (black) and **PBT-NMe$_3$** (orange) in solution; and **D**) PL spectra of nonannealed films on quartz of **PBT-Br** (black), **PBT-Br** after 20 h (dashed black) of exposure to trimethylamine gas, and the corresponding spectra of annealed films of **PBT-Br** (orange), **PBT-Br** after 20 h (dashed orange).

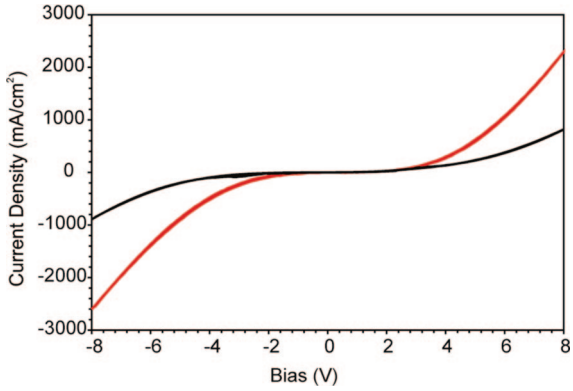

Figure 5. Current density versus bias plots for devices with **PBT-Br**. The measurements on nonannealed films are shown in black, devices with annealed films in red.

ties. It has been shown previously that the response time due to ion motion can be in the order of seconds.[14,19] Therefore, it is possible to suppress the effect of ion motion in polyelectrolytes and, thereby, electron injection by using a recently reported pulsed measurement method.[19] During the scans the bias was pulsed with 500 ms off-times and 5 ms on-time. The result of using this measurement technique on the *J-V* characteristics is shown in Figure 7. Importantly, no light emission is observed under these conditions indicating efficient inhibition of electron injection. Treatment of the data in Figure 7 by the SCLC formalism showed that the hole mobilities were 6.4×10^{-6} cm^2/(V s) and 1.1×10^{-5} cm^2/(V s) for nonannealed and annealed devices, respectively. Hence, the hole mobilities of annealed devices are roughly doubled compared to nonannealed devices. The hole mobilities for devices with **PBT-NMe$_3$** are about 1 order of magnitude lower than for the neutral precursor polymer **PBT-Br**. Significantly, the reported hole-mobilities of **PBT-NMe$_3$** are almost 3 orders of magnitude higher than measurements reported on a commercially available charged polythiophene derivative.[20]

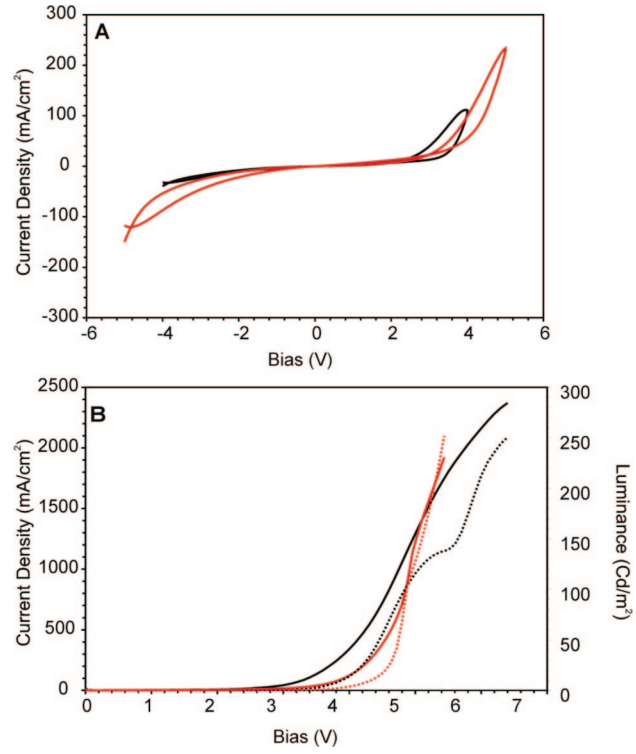

Figure 6. Devices after 20 h of exposure for both nonannealed (black) and annealed (red) films: (A) device characterization under conventional conditions; (B) luminance versus bias plot (dotted lines) obtained using conventional conditions.

Summary and Conclusions

The initial goal of the study was to develop a route to conjugated polyelectrolytes based on the synthetic route in Scheme 1. Our structural design was inspired by previous work on neutral conjugated polymers with high carrier mobilities, thus the interest in the **PBT-Br** to **PBT-NMe$_3$** conversion. However,

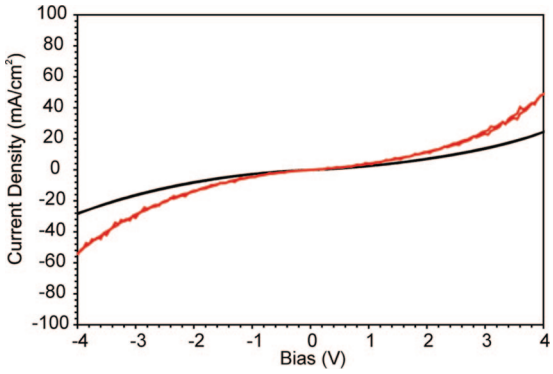

Figure 7. $J-V$ characteristics of devices with **PBT-NMe$_3$** using the pulsed bias technique. The measurements on nonannealed films are shown in black; devices with annealed films are in red.

it was found that the structural features in **PBT-NMe$_3$**, namely the high hydrophobic content with insufficient charged groups, provided for a material that finds little solubility in common solvents. Most significant is that the conjugated backbone retains a high propensity for $\pi-\pi$ stacking and aggregates are formed easily in solution, giving only low solubility in polar solvents. Faced by this limitation we developed a new method of polyelectrolyte formation via in situ quaternization of the alkyl bromide side chains of the neutral precursor polymer. The overall procedure is operationally simple, in that trimethylamine is allowed to diffuse into the precursor film where the in situ reaction takes place. Unreacted amine is easily removed under vacuum.

A series of independent structural characterization techniques supports the proposed structural conversion. In particular high-resolution XPS analysis shows a yield of quaternization of >75% after 20 h of exposure. Diode devices containing **PBT-NMe$_3$** layers show the characteristics of light-emitting electrochemical cells. This observation requires injection of both holes and electrons and, based on the high work function of the electrodes used for device fabrication, indicates the presence of mobile ions. Thus, we anticipate that effective charge injection layers may be incorporated into optoelectronic devices via our new method.

We have also shown that a neutral precursor can be preorganized by spin-coating and annealing. Subsequent in situ quaternization alters the overall morphology of the film as shown by AFM studies. Differences in the absorption spectra and hole mobilities indicate that the initial preorganization can be used to modify optical and electronic couplings in conjugated polyelectrolytes without the need to directly deposit the material from polar solvents. Furthermore, devices containing the in situ obtained CPE film (**PBT-NMe$_3$**) show hole mobilities of up to 1.1×10^{-5} cm^2/(V s). This value is about 3 orders of magnitude higher than that of an anionic polythiophene derivative reported recently.[20] Similar hole mobilities have been reported for polyfluorenes with different counterions.[59] However, these data were derived from conducting AFM measurements, which tend to overestimate mobilities by up to 3 orders of magnitude.[60]

From a broader perspective, the results described herein point to a new chemical method for incorporating polymeric semiconducting materials with an ionic structural component into optoelectronic devices under circumstances where it is not possible to take advantage of commonly used deposition techniques such as spin-coating. A broader class of materials performance may therefore be accessed via this route. Further studies concerning the applicability of in situ conjugated polyelectrolyte formation in different device geometries, such as field-effect transistors and light emitting devices are currently under way.

Experimental Section

General Details. All reactions were carried out under an atmosphere of argon, if not stated otherwise. THF, diethyl ether were dried over sodium/benzophenone and CH_2Cl_2 using calcium hydride. All solvents were stored under inert gas. Dry DMSO and dry chlorobenzene were purchased from Aldrich. N-bromosuccinimide (NBS) was recrystallized from H_2O before use. ^{1}H and ^{13}C NMR spectra were recorded on a Varian UNITY INOVA 400 or 500 MHz spectrometer at room temperature, if not mentioned otherwise. The chemical shifts are given in ppm. Electrospray ionization mass spectrometry (EI-MS) was measured on a VG70 Magnetic Sector instrument. Elemental analysis was done by MSI Analytical Laboratory at the University of California, Santa Barbara. Reactions under microwave heating were done using a Biotage Initiator 2.0 microwave. GPC analysis was conducted with a Waters GPC 2410 against polystyrene standards with THF or DMF as eluent and a refractive index detector. TGA was performed on a Mettler 851e TG and DSC on a TA Instruments DSC Q20. UV/vis spectra were recorded on a Shimadzu UV-2401PC spectrophotometer. Fluorescence measurements were carried out on a PTI Quanta Master luminescence spectrometer.

1-(10-Bromodecyloxy)-4-methoxybenzene (5). 1,10-Dibromodecane (**3**) (39.329 g; 0.1310 mol) was dissolved in acetone (85 mL) and the solution heated to reflux under normal atmosphere. Then a solution of KOH (3.232 g; 0.0576 mol) and methoxyphenol (**4**) (6.505 g; 0.0524 mol) in methanol (85 mL) was added during ~1 h. The resulting suspension was heated to reflux for 30 h. The solvents were removed by rotary evaporation, boiling hexanes (about 500 mL) was added to the residue and the solid filtered off and washed with boiling hexanes one time. After removal of the solvents from the filtrate a white solid was obtained. From this **3** was distilled off in high vacuum leaving a white solid. Column chromatography (silica gel, hexanes/CH_2Cl_2 2/1 increasing to 1/1) afforded **5** as white solid (10.517 g; 0.0306 mol; 59%). ^{1}H NMR (400 MHz, $CDCl_3$): δ 6.84 (s, 4H), 3.91 (t, J = 6.7 Hz, 2H), 3.78 (s, 3H), 3.42 (t, J = 6.7 Hz, 2H), 1.86 (q, J = 7.2 Hz, 2H), 1.76 (q, J = 7.2 Hz, 2H), 1.48−1.41 (m, 4H), 1.38−1.28 (m, 8H). ^{13}C NMR (100 MHz, $CDCl_3$): δ 153.81, 153.45, 115.57, 114.77, 68.78, 55.92, 34.29, 33.01, 29.64, 29.56, 28.93, 28.35, 26.23.

3-(10-(4-Methoxyphenoxy)decyl)thiophene (7). Freshly washed magnesium turnings (1.130 g; 0.0466 mol) and dry diethyl ether (15 mL) were placed in a three necked-flask and the mixture was heated to gentle reflux under argon. A solution of compound **5** (8.000 g; 0.0233 mol) in dry diethyl ether (200 mL) was added dropwise over ~3 h. 3-Bromothiophene (**6**) (4.179 g; 0.0256 mol), [Ni(dppp)Cl_2] (0.126 g; 0.23 mmol), and dry diethyl ether (100 mL) were placed in a second apparatus and the mixture heated to gentle reflux under argon. The resulting Grignard mixture of **5** was then slowly transferred via cannula to the second apparatus under argon. After heating the reaction mixture to reflux for 19 h it was hydrolyzed with cold 0.2 M HCl and extracted with CH_2Cl_2. The organic phases were washed with water until neutral and then dried over $MgSO_4$. The solvents were removed by rotary evaporation giving an orange solid. Purification by column chromatography (silica gel, hexanes/diethyl ether 15/1) afforded **7** as white solid (6.164 g; 0.0178 mol; 76%). ^{1}H NMR (400 MHz, $CDCl_3$): δ 7.24 (dd, J = 4.8 Hz, J = 2.8 Hz, 1H), 6.96−6.92 (m, 2H), 6.84 (s, 4H), 3.91 (t, J = 6.6 Hz, 2H), 3.78 (s, 3H), 2.63 (t, J = 7.8 Hz, 2H), 1.76 (q, J = 6.8 Hz, 2H), 1.63−1.59 (m, 2H), 1.49−1.39 (m, 2H), 1.39−1.26 (m, 10H). ^{13}C NMR (100 MHz, $CDCl_3$): δ 153.80, 153.47, 128.49, 125.24, 119.96, 115.57, 114.77, 68.80, 55.90, 30.75, 30.47, 29.75, 29.71, 29.64, 29.58, 29.52, 26.25. MS (EI): m/z (%) = 346 (35) [M^+], 124 (100) [$OPhOCH_3$], 109 (15), 97 (27).

2-Bromo-3-(10-(4-methoxyphenoxy)decyl)thiophene (8). Compound **7** (2.061 g; 5.95 mmol) was dissolved in THF (13 mL) and the solution cooled to 0 °C. Then NBS (1.071 g; 6.01 mmol) was added slowly in portion. The reaction mixture was stirred for 67 h while slowly warming to room temperature. It was poured into water, extracted with diethyl ether and the organic phase washed with water and dried over $MgSO_4$. Removal of the solvents by

rotary evaporation gave **8** (2.402 g; 5.65 mmol; 95%) without further purification. ^{1}H NMR (400 MHz, $CDCl_3$): δ 7.19 (d, J = 5.8 Hz, 1H), 6.84 (s, 4H), 6.80 (d, J = 5.8 Hz, 1H), 3.89 (t, J = 6.8 Hz, 2H), 3.78 (s, 3H), 2.57 (t, J = 7.8 Hz, 2H), 1.76 (q, J = 7.2 Hz, 2H), 1.62−1.52 (m, 2H), 1.50−1.40 (m, 2H), 1.40−1.26 (m, 10H). ^{13}C NMR (100 MHz, $CDCl_3$): δ 153.86, 153.52, 142.20, 128.49, 125.39, 115.64, 114.82, 109.04, 68.86, 55.98, 29.97, 29.79, 29.73, 29.63, 29.44, 26.29. MS (EI): *m/z* (%) = 428, 426 (20) [M^+], 124 (100) [$OPhOCH_3$], 109 (14), 97 (9).

5,5′-Dibromo-4,4′-bis(10-(4-methoxyphenoxy)decyl)-2,2′-bithiophene (9). Compound **8** (1.674 g; 3.93 mmol), $PdCl_2(PhCN)_2$ (0.045 g; 0.118 mmol), potassium fluoride (0.457 g; 7.86 mmol) and dry DMSO (18 mL) were placed in a three-necked flask equipped with magnetic stirring bar and reflux condenser. The mixture was stirred for 5 min and then silver nitrate (1.335 g; 7.86 mmol) was added in one portion. After stirring at 60 °C for 3 h the some amounts as above of $PdCl_2(PhCN)_2$, potassium fluoride and silver nitrate were added again and the reaction stirred at 60 °C for 18 h. After cooling to room temperature, the reaction mixture was filtered over a plug of silica gel and the residue washed with CH_2Cl_2 (∼250 mL). The filtrate was washed one time with saturated NH_4Cl-solution and three times with H_2O and then dried over $MgSO_4$. The solvent was removed by rotary evaporation giving a reddish solid. Purification by column chromatography (silica gel, hexanes/CH_2Cl_2 2:1 increasing to 1/1) afforded **9** as white solid (1.284 g; 1.51 mmol; 77%). ^{1}H NMR (400 MHz, $CDCl_3$): δ 6.84 (s, 8H), 6.79 (s, 2H), 3.91 (t, J = 6.6 Hz, 4H), 3.78 (s, 6H), 2.53 (t, J = 7.8 Hz, 4H), 1.76 (q, J = 7.2 Hz, 4H), 1.64−1.54 (m, 4H), 1.50−1.40 (m, 4H), 1.40−1.26 (m, 20H). ^{13}C NMR (100 MHz, $CDCl_3$): δ 153.80, 153.46, 143.14, 136.35, 124.64, 115.57, 114.77, 108.05, 68.80, 55.92, 29.82, 29.75,29.67, 29.59, 29.56, 29.37, 26.25. MS (EI): *m/z* (%) = 848 (100) [M^+], 768 (35) [M^+ − Br]. HRMS-EI: *m/z* [M^+] calcd for $C_{42}H_{56}Br_2O_4S_2$, 846.1987; found, 846.1975.

5,5′-Dibromo-4,4′-bis(10-bromodecyl)-2,2′-bithiophene (1). Compound **9** (0.249 g; 0.29 mmol) was dissolved in dry CH_2Cl_2 and the solution heated to reflux. Then boron tribromide (1 M solution in CH_2Cl_2; 0.58 mL; 0.58 mmol) was added in three portions. Each time 0.19 mL of BBr_3 were added and stirred ∼45 min before the next portion was added. Then the reaction mixture was poured into a saturated NH_4Cl solution and extracted with CH_2Cl_2. The organic layer was washed twice with a saturated $NaHCO_3$ solution, twice with H_2O and dried over $MgSO_4$. The solvent was removed by rotary evaporation giving a brown crude product. Purification by column chromatography (silica gel, hexanes) afforded **1** as white/beige solid (0.146 g; 0.19 mmol; 66%). ^{1}H NMR (400 MHz, $CDCl_3$): δ 6.78 (s, 2H), 3.41 (t, J = 6.8 Hz, 4H), 2.52 (t, J = 7.6 Hz, 4H), 1.90−1.78 (m, 4H), 1.62−1.48 (m, 4H), 1.46−1.20 (m, 24H). ^{13}C NMR (100 MHz, $CDCl_3$): δ 143.35, 136.35, 124.65, 108.08, 34.33, 33.02, 29.81, 29.72, 29.60, 29.53, 29.34, 28.95, 28.37. MS (EI): *m/z* (%) = 762 (100) [M^+], 682 (10) [M^+ − Br], 522 (10) [M^+ − 3Br], 351 (11), 271 (10). HRMS-EI: *m/z* [M^+] calcd for $C_{28}H_{42}Br_4S_2$, 757.9461; found, 757.9431.

2,5-Dibromothieno[3,2-*b*]thiophene (11). Thieno[3,2-*b*]thiophene **10** (3.790 g; 0.0270 mol) was dissolved in dry THF (120 mL) at room temperature and the solution cooled to 0 °C. Then NBS (9.820 g; 0.0552 mol) was added in small portions during 1 h at 0 °C. The reaction mixture was stirred for 21 h while slowly warming to room temperature. GC-MS analysis showed full consumption of the starting material. The reaction mixture was poured into cold water (600 mL) and extracted with diethyl ether (5 × 120 mL). The organic layers were washed with water (200 mL) twice and dried over $MgSO_4$. Removal of the solvents gave **11** as white solid (7.650 g; 0.0257 mol; 95%) without further purification. ^{1}H NMR (400 MHz, CD_2Cl_2): δ 7.21 (s, 2H); ^{13}C NMR (100 MHz, $CDCl_3$) δ 138.45, 121.94, 113.81.

2,5-Bis(trimethylstannyl)thieno[3,2-*b*]thiophene (2). Compound **11** (1.632 g; 5.48 mmol) was dissolved dry diethyl ether (250 mL) and the solution cooled to 0 °C. Then *n*-BuLi (2.5 M in hexanes; 5.26 mL; 13.15 mmol) was added dropwise during 1 h and the resulting mixture was stirred for 20 min at 0 °C. Trimethyltin chloride (2.512 g; 12.61 mmol) dissolved in dry diethyl ether (50 mL) was added during 45 min. After 2 h at 0 °C the suspension was poured into H_2O (300 mL), the layers were separated and the aqueous layer was extracted with diethyl ether twice. The combined organic phases were washed with brine twice and dried over $MgSO_4$. Removal of the solvents by rotary evaporation afforded a dark green solid. The crude product was dissolved in benzene (∼30 mL) and treated with activated carbon overnight. The activated carbon was filtered off, the residue washed with benzene and the solvents removed leaving a yellow solid, which was recrystallized from acetonitrile. The purification steps were repeated once to give **2** as white solid (1.212 g; 2.60 mmol; 47%). ^{1}H NMR (400 MHz, CD_2Cl_2): δ 7.27 (s, 2H), 0.39 (s, 18H). ^{13}C NMR (100 MHz, $CDCl_3$): δ 147.64, 141.42, 126.30, −7.99.

Poly(2,5-bis(3-(10-bromodecyl)thiophen-2-yl)thieno[3,2-*b*]thiophene) PBT-Br. Monomer **1** (0.093 g; 0.12 mmol) and monomer **2** (0.057 g; 0.12 mmol) were weighted into a microwave tube, dissolved in dry chlorobenzene (1.3 mL), and the solution was degassed with Argon for 15 min. Then P(*o*-tolyl)$_3$ (0.003 g; 9.9 μmol) and [$Pd_2(dba)_3$] (0.0022 g; 2.4 μmol) were added and the mixture was degassed again for 5 min. The microwave tube was sealed and heated in the microwave with stirring subsequently at 140 °C for 2 min, at 160 °C for 2 min and at 180 °C for 25 min. The reaction time was calculated after the representative temperature had been reached. After the reaction was cooled to 50 °C, a red gel-like precipitate had formed, which was redissolved by addition of chlorobenzene (3 mL) and precipitated from a warm solution into a mixture of methanol (40 mL) and conc. hydrochloric acid (2 mL). The resulting suspension was stirred overnight. The dark-red precipitate was collected by filtration and purified by Soxhlet extraction with acetone, pentane, methanol (each 24 h). The polymer was dissolved again in chlorobenzene and precipitated from a warm solution into methanol to yield **PBT-Br** as dark-red solid (0.078 g; 0.11 mmol; 88%). ^{1}H NMR (500 MHz, $CDCl_3$, T = 50 °C): δ 7.29 (s, 2H), 7.06 (s, 2H), 3.41 (br t, 4H), 2.82 (br t, 4H), 1.92−1.82 (m, 4H), 1.78−1.64 (m, 4H), 1.54−1.25 (m, 24H). Anal. Calcd (%) for $(C_{34}H_{44}Br_2S_4)_n$ (740.78): C, 55.13; H, 5.99. Found: C, 54.53; H, 5.61. GPC (THF): M_n = 13037 g/mol, M_w = 24033 g/mol; PDI = 1.84.

Polyelectrolyte PBT-NMe$_3$. Polymer **PBT-Br** (0.055 g; 0.07 mmol) was dissolved in THF (100 mL) at room temperature and the solution cooled to −78 °C. Condensed trimethylamine (∼2.5 mL) was added dropwise and the solution stirred for 16 h while gradually warming to room temperature. Then THF was removed in vacuo and a 1/1 mixture of THF/EtOH (100 mL) was added and the mixture cooled to −78 °C. After the addition of condensed trimethylamine (∼2.5 mL) the mixture was again stirred for 16 h while gradually warming to room temperature. This process was repeated with EtOH (100 mL) as solvent. Finally, the solvents were removed under reduced pressure leaving a dark red precipitate that was dried at high vacuum overnight. It was dissolved in the minimal amount of DMSO and precipitated into diethyl ether. The resulting suspension was stirred for 24 h and the solid collected by centrifugation. After drying the solid in high vacuum for several days **PBT-NMe$_3$** was obtained as dark red solid (0.073 g; 0.08 mmol; 83%). ^{1}H NMR (400 MHz, d_6-DMSO): δ 7.66 (br s, 2H), 7.34 (br s, 2H), 3.36 (br s, 48H), 3.04 (br s, 18H), 2.80 (br s, 4H), 2.0−1.0 (br, 32H). Anal. Calcd (%) for $(C_{40}H_{62}Br_2N_2S_4)_n$ (859.03): C, 55.93; H, 7.27; N, 3.26. Found: C, 53.12; H, 6.54; N, 2.59.

General Details—Device Fabrication. Samples were prepared on either quartz substrates (spectroscopic measurements) or indium tin oxide (ITO) substrates (electrical measurements) under a nitrogen atmosphere. Substrates were cleaned before use by heating in 70:30 (v/v) H_2SO_4:H_2O_2 solution (quartz only), followed by successive rinsing and ultrasonic treatment in water, acetone, isopropyl alcohol and then drying with N_2 gas and several hours in an oven. The substrates were treated with UV/O_3 prior to polymer deposition. Film thicknesses were measured with an atomic force microcopy (AFM). Scanning probe measurements were preformed using a commercial scanning probe microscope (MultiMode with a Nanoscope Controller IIIa, Veeco Inc.). All scanning probe measurements were done under a dry N_2 atmosphere. Silicon probes

with a spring constant of ~5 N/m and a resonant frequency of ~75 kHz (Budget Sensors) were used for tapping AFM measurements. UV−vis absorption spectra were recorded on a Shimadzu UV-2401 PC diode array spectrometer and fluorescence was measured by using a PTI Quantum Master fluorometer. XPS spectra were recorded on Kratos Axis Ultra XPS system with a base pressure of 1×10^{-10} mbar (UHV), using a monochromated Al Kα X-ray source at $h\nu = 1486$ eV. For electrical measurements current−voltage ($I-V$) measurements were recorded with a Keithley 2602 or 4200 SCS.

Sample Preparation. Samples for all measurements were prepared by first spin coating a solution of poly(3,4-ethylenedioxythiophene) poly(styrenesulfonate) (PEDOT:PSS) (Baytron P 4083, Bayer AG.) on either quartz or ITO substrates yielding approximately 40 nm thick films. The PEDOT:PSS film was then dried at 150 °C for 1 h before spin coating a 80 °C 2% w/v 1,2-dicholorobenzene solution of **PBT-Br** at 800 rpm and using PTFE filters leading to a total film thickness of approximately 120 nm.

Six sets of samples on ITO and quartz substrates were prepared, three annealed and three nonannealed without exposure to trimethylamine gas, with 2 h exposure and with 20 h exposure. Annealed films were heated at 190 °C for 20 min followed by cooling to 30 °C at a 3 °C/min rate. Samples were exposed to a trimethylamine atmosphere by vacuum pumping a desiccator containing the samples for 1 h followed immediate filling with pressurized trimethylamine gas. Samples were exposed to the trimethylamine atmosphere for a selected time followed by vacuum pumping for 20 min to remove excess trimetylamine and immediate transfer to a dry box.

Samples for electrical measurements were deposited with a 100 nm thick gold film electrode (4.9 mm^2 contact area) by thermal evaporation at 10^{-7} Torr (Angstrom Engineering, Inc.) using a shadow mask.

Transport Measurements. For electrical measurements the ITO substrate was bias with a liner increasing/decreasing voltage or step-pulsed voltage using a Keithley 4200 SCS voltage-current sources unit. Voltage measurements were performed with 0.05V steps and 500 ms delay time for linear increasing/decreasing voltage scans and with 500 ms off-times and 5 ms on-times for step-pulsed voltage scans.

Hole mobilities were calculated using the space charge limiting current (SCLC) conduction model:

$$J = \frac{9}{8}\varepsilon_r \varepsilon_o \mu \frac{V^2}{L^3} \quad (1)$$

where ε_r is the dielectric constant of the polymer, ε_o is the vacuum permittivity, μ is the charge mobility, V is the applied voltage, and L is the film thickness.

XPS Measurements. Survey scans between 0 and 500 eV were performed at 0.5 eV steps while high resolution scans of the Br 3d signals (60 eV to 75 eV) were taken at 0.05 eV steps. The C 1s signal was used as reference for the binding energy and assigned at 284.5 eV. The S 2s signals were used for normalization of the intensity signals since no change in composition of S occurs in the polymer upon reaction with trimethylamine. The relative conversion to the CPE was determined by integration of the areas of the two lower and higher binging energy Br 3d signals.

Acknowledgment. The authors are grateful to the NSF (DMR 0606414 and DMR 0547639) and the Institute for Collaborative Biotechnologies for partial support of this work.

References and Notes

(1) Pinto, M. R.; Schanze, K. S. *Synthesis* **2002**, 1293–1309.
(2) Liu, B.; Bazan, G. C. *Chem. Mater.* **2004**, *16*, 4467–4476.
(3) Hara, M. *Polyelectrolytes: Science and Technology*; Marcel Dekker: New York, 1993.
(4) Gaylord, B. S.; Heeger, A. J.; Bazan, G. C. *Proc. Natl. Acad. Sci. U.S.A.* **2002**, *99*, 10954–10957.
(5) Hong, J. W.; Hemme, W. L.; Keller, G. E.; Rinke, M. T.; Bazan, G. C. *Adv. Mater.* **2006**, *18*, 878–882.
(6) Liu, B.; Bazan, G. C. *J. Am. Chem. Soc.* **2006**, *128*, 1188–1196.
(7) Nilsson, K. P. R.; Rydberg, J.; Baltzer, L.; Inganäs, O. *Proc. Natl. Acad. Sci. USA* **2004**, *101*, 11197–11202.
(8) Nilsson, K. P. R.; Herland, A.; Hammarström, P.; Inganäs, O. *Biochemistry* **2005**, *44*, 3718–3724.
(9) Yang, R.; Wu, H.; Cao, Y.; Bazan, G. C. *J. Am. Chem. Soc.* **2006**, *128*, 14422–14423.
(10) Huang, F.; Hou, L.; Shen, H.; Jiang, J.; Wang, F.; Zhen, H.; Cao, Y. *J. Mater. Chem.* **2005**, *15*, 2499–2507.
(11) Wang, L.; Liang, B.; Huang, F.; Peng, J.; Cao, Y. *Appl. Phys. Lett.* **2006**, *89*, 151115/1–3.
(12) Wu, H.; Huang, F.; Mo, Y.; Yang, W.; Wang, D.; Peng, J.; Cao, Y. *Adv. Mater.* **2004**, *16*, 1826–1830.
(13) Ma, W.; Iyer, P. K.; Gong, X.; Liu, B.; Moses, D.; Bazan, G. C.; Heeger, A. J. *Adv. Mater.* **2005**, *17*, 274–277.
(14) Hoven, C.; Yang, R.; Garcia, A.; Heeger, A. J.; Nguyen, T.-Q.; Bazan, G. C. *J. Am. Chem. Soc.* **2007**, *129*, 10976–10977.
(15) Shen, H.; Huang, F.; Hou, L.; Wu, H.; Cao, W.; Yang, W.; Cao, Y. *Synth. Met.* **2005**, *152*, 257–260.
(16) Wu, H. B.; Huang, F.; Peng, J. B.; Cao, Y. *Org. Electron.* **2005**, *6*, 118–128.
(17) Edman, L.; Pauchard, M.; Liu, B.; Bazan, G.; Moses, D.; Heeger, A. J. *Appl. Phys. Lett.* **2003**, *82*, 3961–3963.
(18) Pei, Q. B.; Yu, G.; Zhang, C.; Yang, Y.; Heeger, A. J. *Science* **1995**, *269*, 1086–1088.
(19) Garcia, A.; Yang, R.; Jin, Y.; Walker, B.; Nguyen, T.-Q. *Appl. Phys. Lett.* **2007**, *91*, 153502/1–3.
(20) Garcia, A.; Nguyen, T.-Q. *J. Phys. Chem. C* **2008**, *112*, 7054–7061.
(21) McCulloch, I.; Heeney, M.; Bailey, C.; Genevicius, K.; MacDonald, I.; Shkunov, M.; Sparrowe, D.; Tierney, S.; Wagner, R.; Zhang, W.; Chabinyc, M. L.; Kline, R. J.; McGehee, M. D.; Toney, M. F. *Nat. Mat.* **2006**, *5*, 328–333.
(22) McCullough, R. *Adv. Mater.* **1998**, *10*, 93–116.
(23) Liu, B.; Bazan, G. C. *J. Am. Chem. Soc.* **2004**, *126*, 1942–1943.
(24) Ganem, B., Jr. *Tetrahedron Lett.* **1974**, *11*, 917–920.
(25) Masui, K.; Ikegami, H.; Mori, A. *J. Am. Chem. Soc.* **2004**, *126*, 5074–5075.
(26) Takahashi, M.; Masui, K.; Sekiguchi, H.; Kobayashi, N.; Mori, A.; Funahashi, M.; Tamaoki, N. *J. Am. Chem. Soc.* **2006**, *128*, 10930–10933.
(27) Bäuerle, P.; Würthner, F.; Heid, S. *Angew. Chem., Int. Ed.* **1990**, *29*, 419–420.
(28) Buckel, F.; Persson, P.; Effenberger, F. *Synthesis* **1999**, *6*, 953–958.
(29) Wang, J.; Pappalardo, M.; Keene, F. R. *Aust. J. Chem.* **1995**, *48*, 1425–1436.
(30) Ziegler, K.; Weber, H. *Chem. Ber.* **1937**, *70*, 1275–1279.
(31) Iraqi, A.; Crayston, J. A.; C Walton, J. *J. Mater. Chem.* **1995**, *5*, 1831–1836.
(32) Paganin, L.; Lanzi, M.; Costa-Bizzarri, P.; Bertinelli, F.; Masi, C. *Macromol. Symp.* **2004**, *218*, 11–20.
(33) Fuller, L. S.; Iddon, B.; Smith, K. A. *J. Chem. Soc., Perkin Trans. 1* **1997**, 3465–3470.
(34) Jung, S.-H.; Kim, H. K.; Kim, S.-H.; Kim, Y. H.; Jeoung, S. C.; Kim, D. *Macromolecules* **2000**, *33*, 9277–9288.
(35) Sato, M.; Asami, A.; Maruyama, G.; Kosuge, M.; Nakayama, J.; Kumakura, S.; Fujihara, T.; Unoura, K. *J. Organomet. Chem.* **2002**, *654*, 56–65.
(36) Tierney, S.; Heeney, M.; McCulloch, I. *Synth. Met.* **2005**, *148*, 195–198.
(37) Lidström, P.; Tierney, J.; Wathey, B.; Westman, J. *Tetrahedron* **2001**, *57*, 9225–9283.
(38) Ortony, J. H.; Yang, R.; Brzezinski, J. Z.; Edman, L.; Nguyen, T.-Q.; Bazan, G. C. *Adv. Mater.* **2008**, *20*, 298–302.
(39) Chabinyc, M. L.; Toney, M. F.; Kline, R. J.; McCulloch, I.; Heeney, M. *J. Am. Chem. Soc.* **2007**, *129*, 3226–3237.
(40) DeLongchamp, D. M.; Kline, R. J.; Lin, E. K.; Fischer, D. A.; Richter, L. J.; Lucas, L. A.; Heeney, M.; McCulloch, I.; Northrup, J. E. *Adv. Mater.* **2007**, *19*, 833–837.
(41) Kline, R. J.; DeLongchamp, D. M.; Fischer, D. A.; Lin, E. K.; Richter, L. J.; Chabinyc, M. L.; Toney, M. F.; Heeney, M.; McCulloch, I. *Macromolecules* **2007**, *40*, 7960–7965.
(42) Gaylord, B. S.; Wang, S. J.; Heeger, A. J.; Bazan, G. C. *J. Am. Chem. Soc.* **2001**, *123*, 6417–6418.
(43) http://srdata.nist.gov/xps/Bind_E.asp.
(44) Moulder, J. F.; Stickle, W. E.; Sobol, P. E.; Bomben, K. D. In *Handbook of X-ray Photoelectron Spectroscopy*; Chastian, J., Ed.; Perkin-Elmer Corp.: Eden Prairie, MN, 1979.
(45) Kline, R. J.; McGehee, M. D.; Kadnikova, E. N.; Liu, J.; Frechet, J. M. J. *Adv. Mater.* **2003**, *15*, 1519–1522.
(46) Yang, H.; Shin, T. J.; Yang, L.; Cho, K.; Ryu, C. Y.; Bao, Z. *Adv. Funct. Mater.* **2005**, *15*, 671–676.
(47) Sirringhaus, H.; Brown, P. J.; Friend, R. H.; Nielsen, M. M.; Bechgaard, K.; Langeveld-Voss, B. M. W.; Spiering, A. J. H.; Janssen,

R. A. J.; Meijer, E. W.; Herwig, P.; de Leeuw, D. M. *Nature* **1999**, *401*, 685–688.
(48) Williams, D.; Fleming, I. *Spectroscopic Methods in Organic Chemistry*, McGraw-Hill: Maidenhead, U.K., 1995.
(49) Heeney, M.; Bailey, C.; Genevicius, K.; Shkunov, M.; Sparrowe, D.; Tierney, S.; McCulloch, I. *J. Am. Chem. Soc.* **2005**, *127*, 1078–1079.
(50) Ong, B. S.; Wu, Y.; Liu, P.; Gardner, S. *J. Am. Chem. Soc.* **2004**, *126*, 3378–3379.
(51) Zen, A.; Pflaum, J.; Hirschmann, S.; Zhuang, W.; Jaiser, F.; Asawapirom, U.; Rabe, J. P.; Scherf, U.; Neher, D. *Adv. Funct. Mater.* **2004**, *14*, 757–764.
(52) Becker, R. S.; Melo, J. S. D.; Macüanita, A. L.; Elisei, F. *J. Phys. Chem.* **1996**, *100*, 18683–18695.
(53) Cagnoli, R.; Mucci, A.; Parenti, F.; Schenetti, L.; Borsari, M.; Lodi, A.; Ponterini, G. *Polymer* **2006**, *47*, 775–784.
(54) Goh, C.; Kline, R. J.; McGehee, M. D.; Kadnikova, E. N.; Frechet, J. M. J. *Appl. Phys. Lett.* **2005**, *86*, 122110/1–3.
(55) Koch, N.; Kahn, A.; Ghijsen, J.; Pireaux, J.-J.; Schwartz, J.; Johnson, R. L.; Elschner, E. *Appl. Phys. Lett.* **2003**, *82*, 70–72.
(56) The LUMO energies of **PBT-Br** and **PBT-NMe$_3$** were estimated to be -3.1 ± 0.5 eV by relation to the LUMO energy of **PBT** (-3.1 eV) and the fact that conjugated polyelectrolytes show similar LUMO energies as their neutral counterparts to within $\pm$ 0.3 eV. See: (a) Parmer, J. E.; Mayer, A. C.; Hardin, B. E.; Scully, S. R.; McGehee, M. D.; Heeney, M.; McCulloch, I. *Appl. Phys. Lett.* **2008**, *92*, 113309. (b) Seo, J. H.; Nguyen, T. Q. *J. Am. Chem. Soc.* **2008**, *130*, 10042–10043.
(57) Coropceanu, V.; Cornil, J.; Filho, D. A. d. S.; Olivier, Y.; Silbey, R.; Brédas, J. L. *Chem. Rev.* **2007**, *107*, 926–952.
(58) Edman, L. *Electrochim. Acta* **2005**, *50*, 3878–3885.
(59) Yang, R.; Garcia, A.; Korystov, D.; Mikhailovsky, A.; Bazan, G. C.; Nguyen, T.-Q. *J. Am. Chem. Soc.* **2006**, *128*, 16532–16539.
(60) Reid, O. G.; Munechika, K.; Ginger, D. S. *Nano Lett.* **2008**, *8*, 1602–1609.

MA802139J